

KfK 2899  
September 1979

# **Recent Work on Structural-Material Cross Sections at Kernforschungszentrum Karlsruhe**

F. H. Froehner, K. Wisshak, F. Kaeppler  
Institut für Angewandte Kernphysik  
Institut für Neutronenphysik und Reaktortechnik  
Projekt Schneller Brüter

**Kernforschungszentrum Karlsruhe**



KERNFORSCHUNGSZENTRUM KARLSRUHE

Institut für Angewandte Kernphysik  
Institut für Neutronenphysik und Reaktortechnik  
Projekt Schneller Brüter

KfK 2899

Recent Work on Structural-Material Cross Sections  
at Kernforschungszentrum Karlsruhe

---

F.H. Fröhner, K. Wisshak, F. Käppler

Contribution to the Topical Discussion on "Progress in Neutron Data  
of Structural Materials for Fast Reactors since the NEANDC/NEACRP  
Specialist Meeting at CBNM Geel in December 1977", 21st NEANDC Meeting,  
26 September 1979 at Geel

Kernforschungszentrum Karlsruhe GmbH, Karlsruhe

Als Manuskript vervielfältigt  
Für diesen Bericht behalten wir uns alle Rechte vor

Kernforschungszentrum Karlsruhe GmbH  
ISSN 0303-4003

## Abstract

- (1) In order to clarify a rather confused issue the neutron capture cross section of  $^{56}\text{Fe}$  between 16 and 60 keV was remeasured relative to gold under very clean conditions at the Karlsruhe Van de Graaff accelerator. The metallic samples were isotopically pure and very thin (0.15, 0.3 and 0.6 mm). Time-of-flight discrimination between capture photons and scattered neutrons was employed to suppress signals due to capture of resonance-scattered neutrons outside the sample. This novel technique improves the accuracy significantly with which s-wave resonance capture of structural materials can be measured. The controversial radiation width of the 27.7 keV resonance was found to be  $\Gamma_{\gamma} = 1.00 \pm 0.05$  eV (value not quite final yet).
- (2) An attempt was made to understand the disconcerting discrepancies between the resonance parameters for  $^{58}\text{Fe}+n$  determined at Karlsruhe and at Oak Ridge.
- (3) Statistical resonance parameters for the stable chromium, iron and nickel isotopes were recalculated with an improved version of the maximum-likelihood estimation program STARA. Both strength functions and level spacings differ slightly from the previously (1977) reported values, level spacings being systematically higher.
- (4) A comparison of the total cross section across the 24.4 keV window of  $^{56}\text{Fe}+n$  recently measured at BNL showed good consistency with Harvey's 1970 data for natural iron and with the 1977 KEDAK evaluation.

Neue Arbeiten über Strukturmaterial-Wirkungsquerschnitte im  
Kernforschungszentrum Karlsruhe

Zusammenfassung

- (1) Um eine ziemlich verworrene Situation zu klären, wurde der Neutroneneinfang-Querschnitt von  $^{56}\text{Fe}$  zwischen 16 und 60 keV am Karlsruher Van-de-Graaff-Beschleuniger neu vermessen, relativ zu Gold und unter besonders sauberen Versuchsbedingungen. Die metallischen Proben waren isotopisch rein und sehr dünn (0.15, 0.3 und 0.6 mm). Flugzeit-Diskriminierung zwischen Einfangphotonen und Streuneutronen ermöglichte völlige Unterdrückung der Signale, die vom Einfang resonanzgestreuter Neutronen außerhalb der Probe herrühren. Mit diesem neuen Verfahren kann s-Wellen-Resonanzeinfang in Strukturmaterialien wesentlich genauer als bisher gemessen werden. Für die umstrittene Strahlungsbreite der 27.7-keV-Resonanz wurde  $\Gamma_{\gamma} = 1.00 \pm 0.05$  eV gefunden (Wert noch nicht ganz endgültig).
- (2) Es wurde versucht, die beunruhigenden Diskrepanzen zwischen den Resonanzparametern für  $^{58}\text{Fe}+n$  aus Karlsruhe und Oak Ridge zu verstehen.
- (3) Niveaustatische Parameter für die stabilen Chrom-, Eisen- und Nickel-Isotope wurden neu gerechnet mit einer verbesserten Version des Programms STARA zur Parameterschätzung nach der Methode der größten Mutmaßlichkeit. Sowohl Stärkefunktionen als auch mittlere Niveauabstände unterscheiden sich leicht von den 1977 veröffentlichten Werten, wobei die Niveauabstände systematisch höher sind.
- (4) Ein Vergleich des kürzlich am BNL gemessenen Gesamtquerschnitts über das 24.4-keV-Fenster von  $^{56}\text{Fe}+n$  ergab gute Konsistenz mit Harveys Daten für natürliches Eisen von 1970 und mit der KEDAK-Auswertung von 1977.

1. Determination of  $\Gamma_\gamma$  for the 27.7 keV Resonance of  $^{56}\text{Fe}+n$  with a New Technique

Table 1, showing radiation widths obtained for the famous 27.7 keV resonance of  $^{56}\text{Fe}+n$  (Refs. 1 - 5), illustrates the limited success achieved after more than a decade of effort to determine the capture cross sections of structural materials. Especially s-wave resonances are difficult to measure because even near their peaks capture is about three orders of magnitude less probable than scattering. One must therefore use rather thick samples to get sufficient statistics, which means large multiple-scattering corrections

(1) from the sample itself,

(2) from the vicinity of the sample including the detector.

Especially the latter corrections are difficult to estimate, requiring Monte Carlo calculations with detailed modelling of the structures near the sample. In all past time-of-flight experiments the primary flight path was long compared to the additional secondary flight paths of scattered neutrons. Hence for a given resonance the capture events corresponding to (1) and (2) were recorded almost simultaneously with the first-collision (primary) capture events, as shown in Fig. 1.

Not much can be done about this at linacs. Pulsed Van de Graaff accelerators, on the other hand, admit flight paths comparable with, or even shorter than, the distances between the sample and nearby structures. This and the possibility to tailor the neutron spectrum allows efficient time-of-flight discrimination against all neutron capture outside the sample (Fig. 2).

Consider for example the novel geometry chosen at KfK for the recent re-measurement of the 27.7 keV resonance of  $^{56}\text{Fe}+n$  (Fig. 3). The primary flight path was only 8 cm long, about half as long as the distance between the sample and the detector. Scattered 27.7 keV neutrons can be captured in the lead shield or the detector not sooner than 40 - 70 ns after registration of the capture photons. Consequently the signals corresponding

to (2) occur far removed from the 27.7 keV peak which is only a few ns wide (Fig. 2).

Scattering from other s-wave resonances was eliminated completely by adjusting the accelerator voltage so as to produce  ${}^7\text{Li}(p,n)$  neutrons only with energies between 10 and 60 keV, all of them emitted into a cone with  $60^\circ$  opening angle. The capture detector was placed outside this cone and thus did not see any primary neutrons.

Three metallic, uncanned disc samples of isotopically pure  ${}^{56}\text{Fe}$  were used. The thicknesses were 0.15, 0.3 and 0.6 mm, whereas the thinnest sample used up to now was 0.5 mm thick (see Table 1). The reference sample was a gold disc, 0.25 mm thick. The detector response to a pure scatterer was checked with a graphite sample.

The main advantages over past experiments are listed in Table 2. Figs. 4 and 5 show superimposed sample-in and sample-out time-of-flight spectra for the thinnest and the thickest sample. Signal-to-background ratio, statistics and resolution are seen to be quite adequate for background subtraction and resonance analysis of the 27.7 keV s-wave level.

Fig. 6 shows the fits obtained with the automatic shape analysis program FANAC (Ref. 6). Within 2 % all three samples gave the same radiation width for the 27.7 keV resonance. The p-wave peaks below and above were calculated with fixed parameters taken from Ref. 6. A similarly good fit to the data was obtained with the p-wave parameters recommended in Ref. 7 and a slightly (2 %) higher  $\Gamma_\gamma$  for the 27.7 keV resonance. The multiple-scattering contribution (dashed lines) is seen to be unproblematic for all three samples. The results given in Fig. 6 are not quite final yet as small corrections are still missing for photon self-absorption in the sample and for deviations from the ideal linear relationship between Moxon-Rae detector efficiency and excitation energy. The combined effect is expected to be few percent at most. The errors given in Fig. 6 include statistical, background subtraction, resonance analysis and normalization (ENDF/B-IV gold cross section) errors.

We conclude that the new technique of secondary flight time discrimination

and spectrum tailoring efficiently removes the problem of neutron sensitivity of the detector system. This and the much thinner samples compared to previous measurements reduce the uncertainties of  $\Gamma_\gamma$  and of  $\sigma_\gamma$  to well below 10 %.

## 2. Comparison of Resonance Parameter Sets for $^{58}\text{Fe}+n$

Fairly comprehensive sets of resonance parameters for  $^{58}\text{Fe}+n$  were reported for the first time in 1976 from KfK (Ref. 8) and subsequently from Albany/ORNL (Ref. 9). A comparison of the two parameter sets reveals serious discrepancies for the s-wave resonances, see Table 3, although both groups had measured transmission of iron oxide samples with comparable enrichment in  $^{58}\text{Fe}$ . Both analyzed the data with essentially the same multi-level R-function formalism. The resolution was better at ORNL but quite adequate for the s-wave resonances at KfK (see Fig. 7). Two sample thicknesses had been used at KfK, only one at ORNL. The conspicuous difference in  $R'$ , the effective scattering radius, cannot be explained by the different treatment of distant levels. The cross sections for oxygen,  $^{54}\text{Fe}$  and  $^{56}\text{Fe}$  employed in the resonance analyses were also quite similar. The goodness of fit in Fig. 7 looks satisfactory while that of Ref. 9 could not be judged equally well from the figures given there. We therefore calculated the theoretical transmissions expected for the KfK measurements with the parameters of Ref. 4. An example is shown in Fig. 8. The experimental data are not fitted as well as with the KfK parameters ( $\chi^2 = 1233$  for 509 degrees of freedom instead of  $\chi^2 = 648$ ), potential scattering being too high, the 43 keV resonance too narrow. Similar differences between fits from both groups were also observed in the past for  $^{54}\text{Fe}+n$  (Refs. 10, 11). The Albany/ORNL results seem to indicate a fitting procedure less efficient than the fully automatic, iterative parameter adjustment employed in the KfK R-matrix code FANAL (Ref. 12). On the other hand the  $^{58}\text{Fe}$  transmission minima are not quite accurately reproduced by the KfK curves either. The theoretical  $^{58}\text{Fe}$  s-wave cross section there is equal to the unitarity limit,  $4\pi\lambda^2$ , within a fraction of a percent, and the small imperfection of the fit must be due to too much background subtracted or too low cross section calculated for the sample impurities ( $^{54}\text{Fe}$  and  $^{56}\text{Fe}$ ) or slightly wrong sample assay. Since this error is obviously less important it is

concluded that the KfK values for  $\Gamma_n$  and  $R'$  are closer to the truth than those of Ref. 9.

### 3. Revised Strength Functions and Average Level Spacings for Cr, Fe and Ni Isotopes

The statistical resonance analysis program STARA simultaneously estimates strength functions  $S$  and average level spacings  $D$  corrected for missing levels, from observed resonance energies and neutron widths. For  $s$ -wave levels of given spin, for instance,  $\langle \Gamma_n^0 \rangle = SD$  and  $D$  are obtained as solution of the maximum-likelihood equations (Ref. 13)

$$\langle \Gamma_n^0 \rangle \left( 1 + \frac{1}{N} \sum_{\lambda} \frac{2}{\sqrt{\pi}} \frac{e^{-x_{\lambda}} \sqrt{x_{\lambda}}}{u - \operatorname{erfc} \sqrt{x_{\lambda}}} \right) = \bar{\Gamma}_n^0 ,$$

$$\frac{1}{N} \sum_{\lambda} \frac{\operatorname{erfc} \sqrt{x_{\lambda}}}{u - \operatorname{erfc} \sqrt{x_{\lambda}}} = 1$$

where  $u \equiv (c_1 + 2c_2 E_L)D$  ,  $x_{\lambda} \equiv \frac{(\Gamma_n^0)_{\lambda}}{2\langle \Gamma_n^0 \rangle}$  .

The  $(\Gamma_n^0)_{\lambda}$  are the reduced neutron widths,  $\bar{\Gamma}_n^0$  is the sample average,  $E_L$  the lower boundary of the energy interval considered,  $c_1$  and  $c_2$  are coefficients of a parabolic fit to the staircase curve giving the number of observed levels as a function of energy. This nonlinear system of equations must be solved by iteration. The numerical iterative procedure as well as the estimation of confidence limits was recently improved over an older version of the code. Previously reported results (Refs. 3, 14) were recalculated with the new code version. The results are shown in Table 4. They should be considered as superseding those of Refs. 3 and 14. Fig. 9 shows the strength functions plotted together with theoretical results of Müller and Rohr (Ref. 16) as a function of nucleon number.

4. Comparison of New Data for the Window in the Total Cross Section of Iron at 24.4 keV with Older Data

The total cross section across the important interference minimum ("window") at 24.4 keV belonging to the 27.7 keV resonance of  $^{56}\text{Fe}+n$  was recently measured at the RPI linac with an isotopically pure, 69 cm thick sample of  $^{56}\text{Fe}$  (Ref. 17). Fig. 10 shows excellent consistency between the new results and those obtained with a 51 cm thick natural-iron sample by Harvey (Ref. 18). KEDAK point cross sections (Ref. 3) calculated from evaluated resonance parameters without "smooth" component are also seen to be in satisfactory agreement with both experimental data sets.

References

1. R.W. Hockenbury, Z.M. Bartolome, J.R. Tatarczuk, W.R. Moyer and R.C. Block, Phys. Rev. 178(1969)1746
2. A. Ernst, F.H. Fröhner, D. Kompe, Nuclear Data for Reactors, IAEA Vienna (1970), vol. I, p. 633
3. F.H. Fröhner, 1977 Geel Meeting on Neutron Data of Structural Materials for Fast Reactors, Pergamon Press (1979), p. 138
4. B.J. Allen and A.R. de L. Musgrove, 1977 Geel Meeting on Neutron Data of Structural Materials for Fast Reactors, Pergamon Press (1979), p. 447
5. D.B. Gayther, B.W. Thomas, B. Thom, M.C. Moxon, 1977 Geel Meeting on Neutron Data of Structural Materials for Fast Reactors, Pergamon Press (1979), p. 547
6. F.H. Fröhner, Report KfK 2145 (1977)
7. F.G. Perey, G.T. Chapman, W.E. Kinney, C.M. Perey, 1977 Geel Meeting on Neutron Data of Structural Materials for Fast Reactors, Pergamon Press (1979), p. 530
8. H. Beer, Li Dy Hong, F. Käppeler, Report KfK 2337 (1976); Nucl. Sci. Eng. 67(1978)184
9. J.B. Garg, S. Jain, J.A. Harvey, Phys. Rev. C18(1978)1441
10. H. Beer, R.R. Spencer, Nucl. Phys. A240(1975)29
11. M.S. Pandey, J.B. Garg, J.A. Harvey, W.M. Good, Nuclear Cross Sections and Technology, Washington 1975, NBS Spec. Publ. 425, Vol. 2, p. 748
12. F.H. Fröhner, Report KfK 2129 (1976)
13. F.H. Fröhner, Report KfK 2669 (1979), pp. 63-65

14. F.H. Fröhner, Neutron Physics and Nuclear Data, Harwell (1978), p. 268
15. D.B. Syme, P.H. Bowen, Neutron Physics and Nuclear Data, Harwell (1978), p. 319
16. K.N. Müller, G. Rohr, Report KfK 1114 (1969), Nucl. Phys. A164(1971)97
17. H.J. Liou, R.E. Chrien, R.C. Block, U.N. Singh, Nucl. Sci. Eng. 70 (1979) 150
18. J.A. Harvey, National Topical Meeting on New Developments in Reactor Physics and Shielding, Kiamesha Lake (1972), CONF-720901, vol. 2, p. 1075

Table 1 Radiation Widths for the 27.7 keV Resonance of  $^{56}\text{Fe}+n$

Reference	Sample Thickness (Fe at./b)		$\Gamma_{\gamma}$ (eV)
Hockenbury + (1969) /1/	$5.4 \cdot 10^{-2}$	} $\text{Fe}_2\text{O}_3$	1.44±0.14
	$6.3 \cdot 10^{-3}$		
Ernst + (1970) /2/	$9.9 \cdot 10^{-3}$	$\text{Fe}_2\text{O}_3$	1.4±0.2 a)
Fröhner (1977) /3/	(reanalysis)		1.25±0.20 b)
Allen + (1977) /4/	$8.2 \cdot 10^{-3}$	$^{56}\text{Fe}$	1.6±0.3
Gayther + (1977) /5/	$1.7 \cdot 10^{-2}$	$^{56}\text{Fe}$	1.05±0.02 c)
	$4.1 \cdot 10^{-2}$	"	0.73±0.06 c)
Wisshak + (1979) (present work)	$5.28 \cdot 10^{-3}$	$^{56}\text{Fe}$	0.98±0.04 c)
	$2.65 \cdot 10^{-3}$	"	1.00±0.05 c)
	$1.38 \cdot 10^{-3}$	"	0.99±0.07 c)

a) SLBW area analysis, superseded

b) Reich-Moore shape analysis

c) preliminary

Table 2

Main Advantages of the Present Set-up:

1. High neutron flux due to short flight path (8 cm) allows use of very thin samples  
→ small multiple scattering.
2. Absence of other masses near the sample makes flight paths of scattered neutrons large  
→ efficient time-of-flight discrimination against capture of scattered neutrons outside the sample.
3. Tailored spectrum (10 - 60 keV)  
→ no background from other s-wave resonances.
4. Good time resolution (1.2 ns)  
→ sufficient energy resolution for resonance analysis even with 8 cm flight path.

Table 3

<sup>58</sup>Fe+n , s-wave resonances

E <sub>0</sub> (keV)	Γ <sub>n</sub> (keV)	
	KfK	Albany/ORNL
10.38	.416±.032	.249±.025
43.15	6.37±.21	4.32±.43
66.9	.997±.049	.81±.08
92.5	12.23±.78	7.43±.74
121.0	2.67±.21	1.81±.18
178.5	2.39±.25	2.75±.28
240.0	10.80±1.40	10.19±1.02
265.0	9.20±1.30	6.96±.70
310.2	3.10±.47	2.90±.29
320.3	1.03±.16	1.77±.18
	R' = 5.6 fm	R' = 7.2 fm

Table 4 Revised level-statistical s-wave parameters for Cr, Fe and Ni isotopes, corrected for missing levels with the maximum-likelihood program STARA /13/. These estimates supersede those in /3/ and /14/.

Target Nucleus	$E_1 - E_2$ (keV)	No. of Levels	$S_0$ ( $10^{-4}$ )	$D_0$ (keV)	Resonance Parameters
$^{50}\text{Cr}$	0-360	20	$2.5 \pm_{0.6}^{1.1}$	$15.8 \pm 1.6$	KEDAK /3/
$^{52}\text{Cr}$	0-420	11	$2.3 \pm_{0.7}^{1.7}$	$37 \pm 7$	"
$^{53}\text{Cr}$	0-250	32	$4.5 \pm_{0.8}^{1.3}$	$5.9 \pm 0.6$	"
$^{54}\text{Cr}$	0-310	11	$1.74 \pm_{0.42}^{0.99}$	$19.4 \pm 4.5$	"
$^{54}\text{Fe}$	0-400	15	$7.6 \pm_{1.8}^{3.8}$	$20.4 \pm 2.7$	"
$^{56}\text{Fe}$	0-400	17	$2.5 \pm_{0.6}^{1.3}$	$21.4 \pm 1.9$	"
$^{57}\text{Fe}$	0-200	22	$4.3 \pm_{0.8}^{1.5}$	$6.5 \pm 0.8$	"
$^{58}\text{Fe}$	0-330	10	$4.5 \pm_{1.2}^{2.9}$	$21.6 \pm 5.6$	KfK /8/
$^{58}\text{Ni}$	0-418	23	$2.9 \pm_{0.7}^{1.3}$	$16.7 \pm 2.1$	Harwell /15/
$^{60}\text{Ni}$	0-400	18	$3.1 \pm_{0.7}^{1.4}$	$14.6 \pm 2.3$	KEDAK /3/
$^{61}\text{Ni}$	0-70	31	$2.9 \pm_{0.6}^{1.0}$	$1.71 \pm 0.19$	"
$^{62}\text{Ni}$	0-400	19	$2.9 \pm_{0.7}^{1.3}$	$18.6 \pm 1.9$	"
$^{64}\text{Ni}$	0-400	18	$3.1 \pm_{0.8}^{1.6}$	$19.9 \pm 2.0$	"

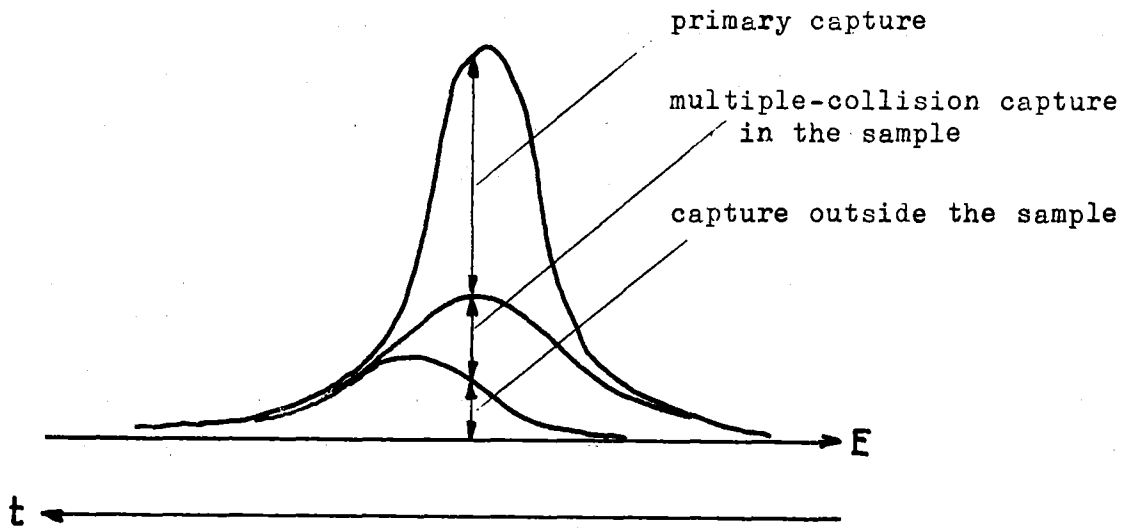


Fig. 1 - Capture peak as seen in conventional time-of-flight experiments: Multiple-collision contributions from within and without the sample occur almost simultaneously with the primary yield.

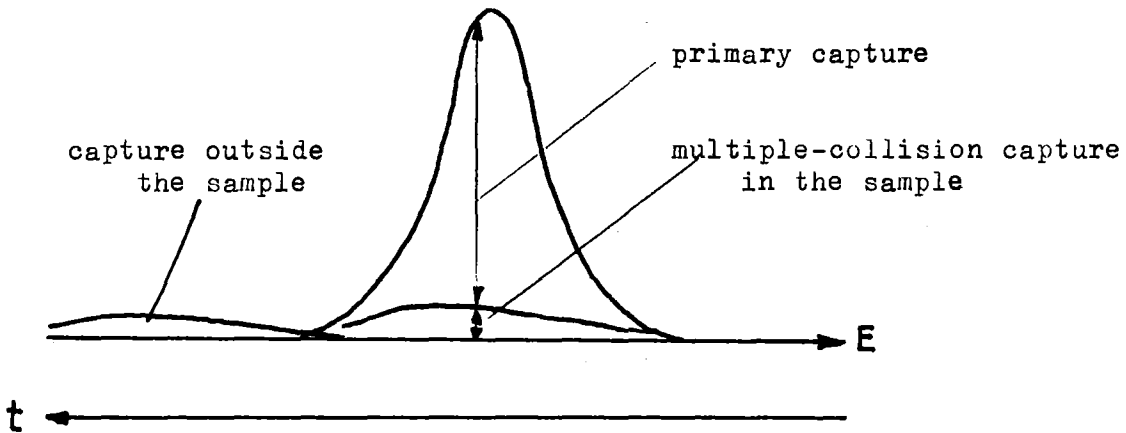


Fig. 2 - Capture peak as observed with the new technique (primary and secondary flight paths of comparable length). Capture outside the sample occurs with time delay, multiple-collision capture is reduced because of thinner sample.

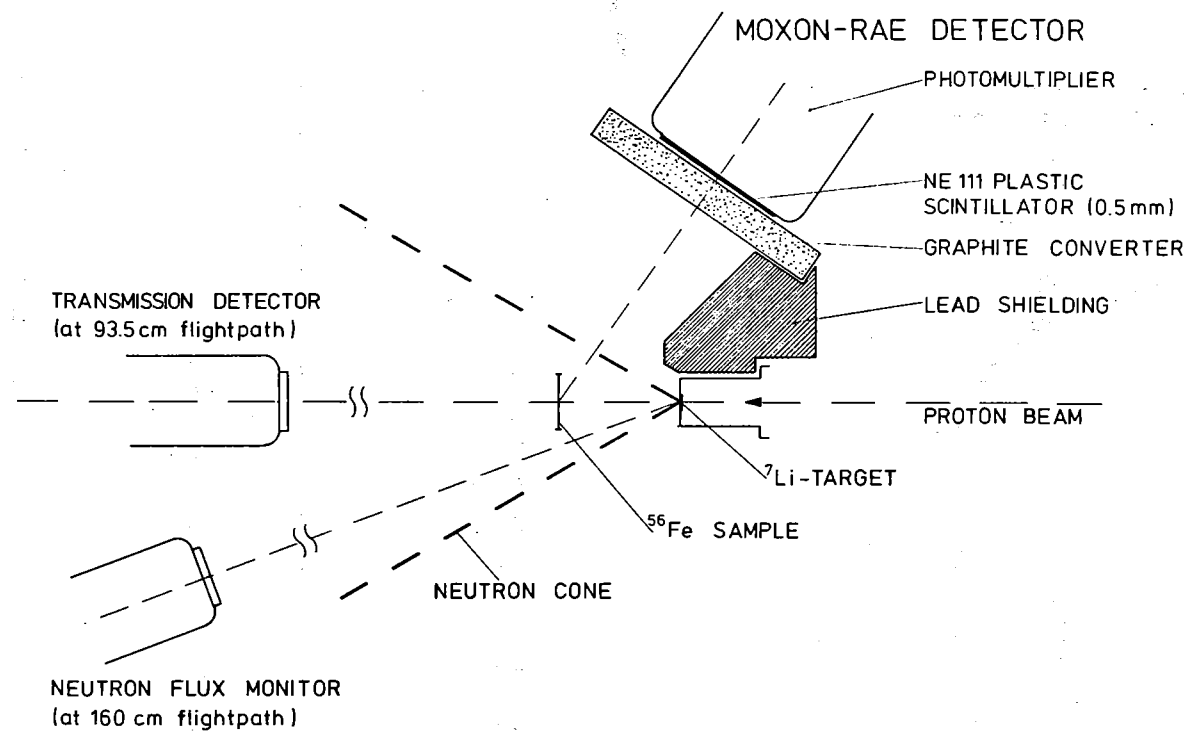


Fig. 3 Schematic Set-up for the Capture Cross Section Measurement on  $^{56}\text{Fe}$

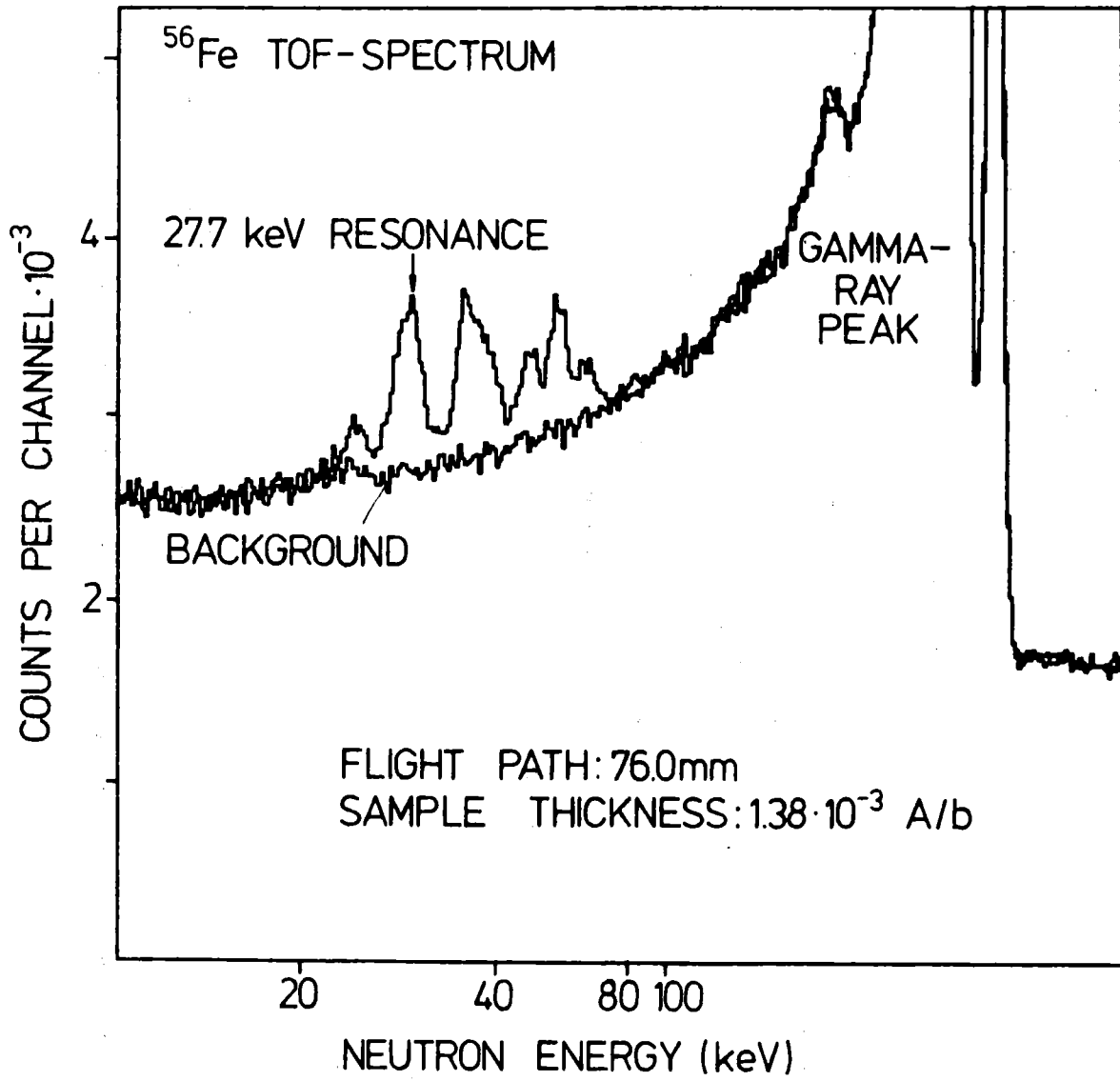


Fig. 4 - Flight-time spectra observed with and without the thinnest  $^{56}\text{Fe}$  sample (0.00138 at./b)

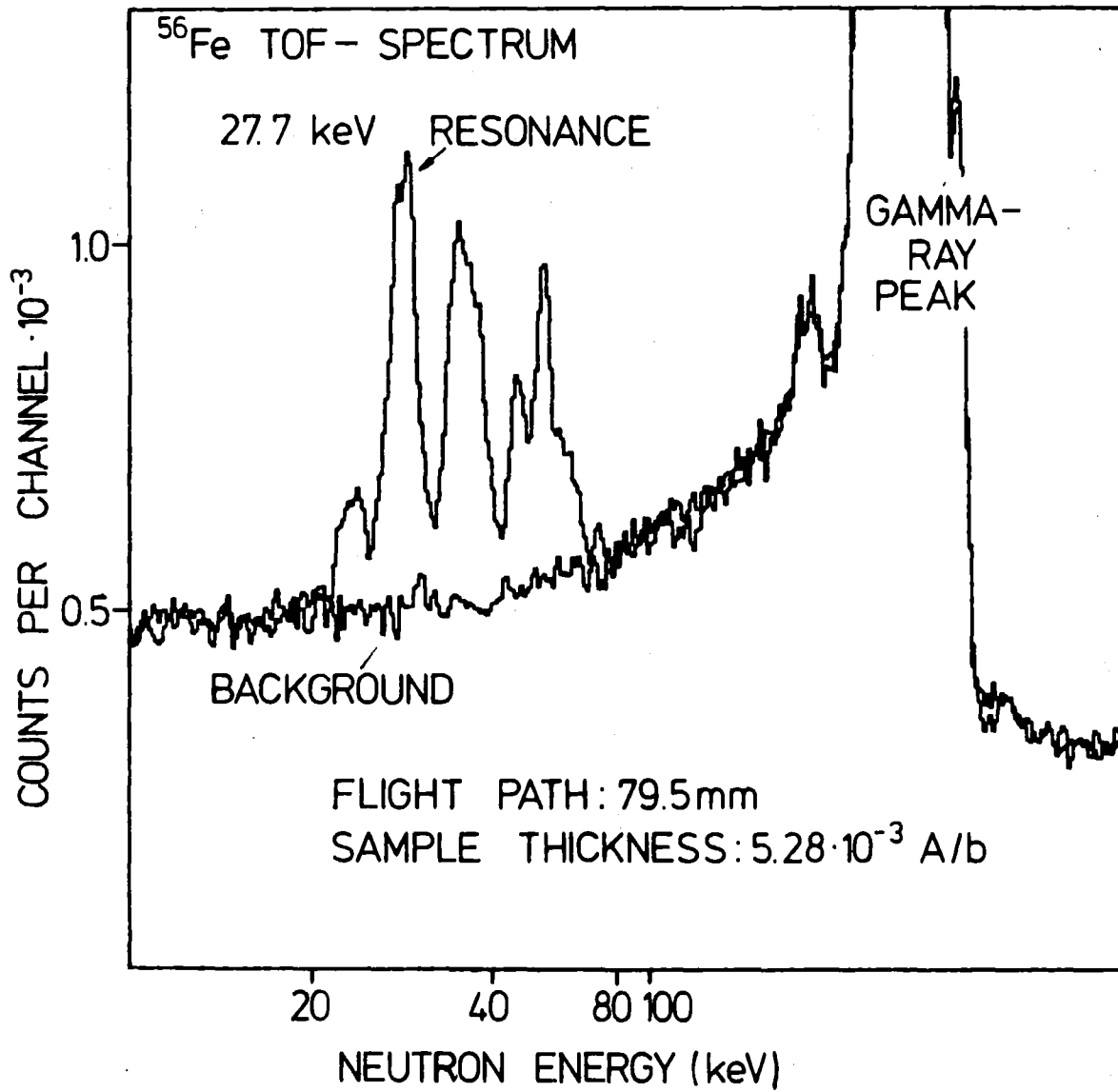


Fig. 5 - Flight-time spectra observed with and without the thickest <sup>56</sup>Fe sample (0.00528 at./b)

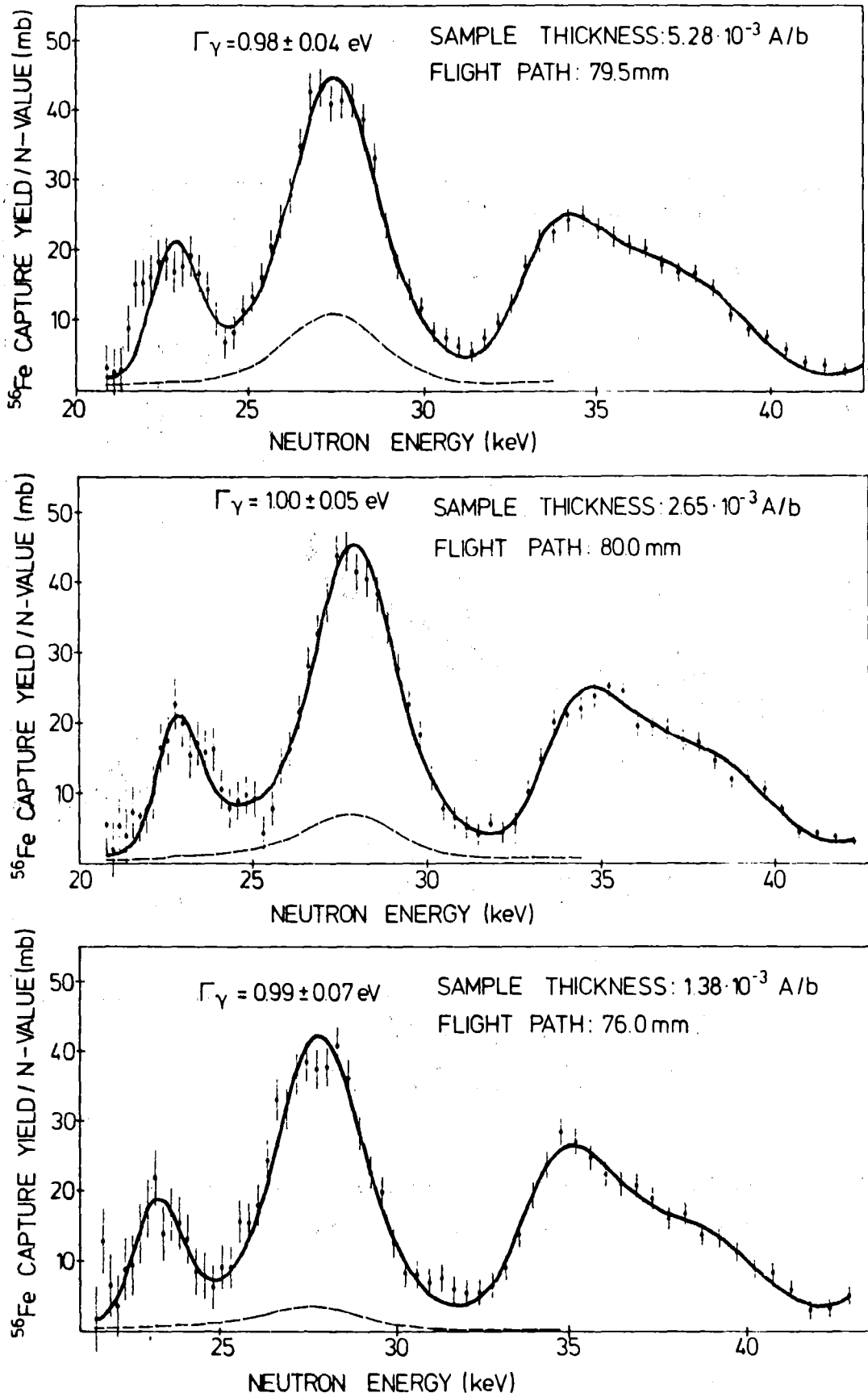


Fig. 6 - FANAC fits to the region around the 27.7 keV resonance of  $^{56}\text{Fe}+n$ . Dashed line: multiple-collision contribution.

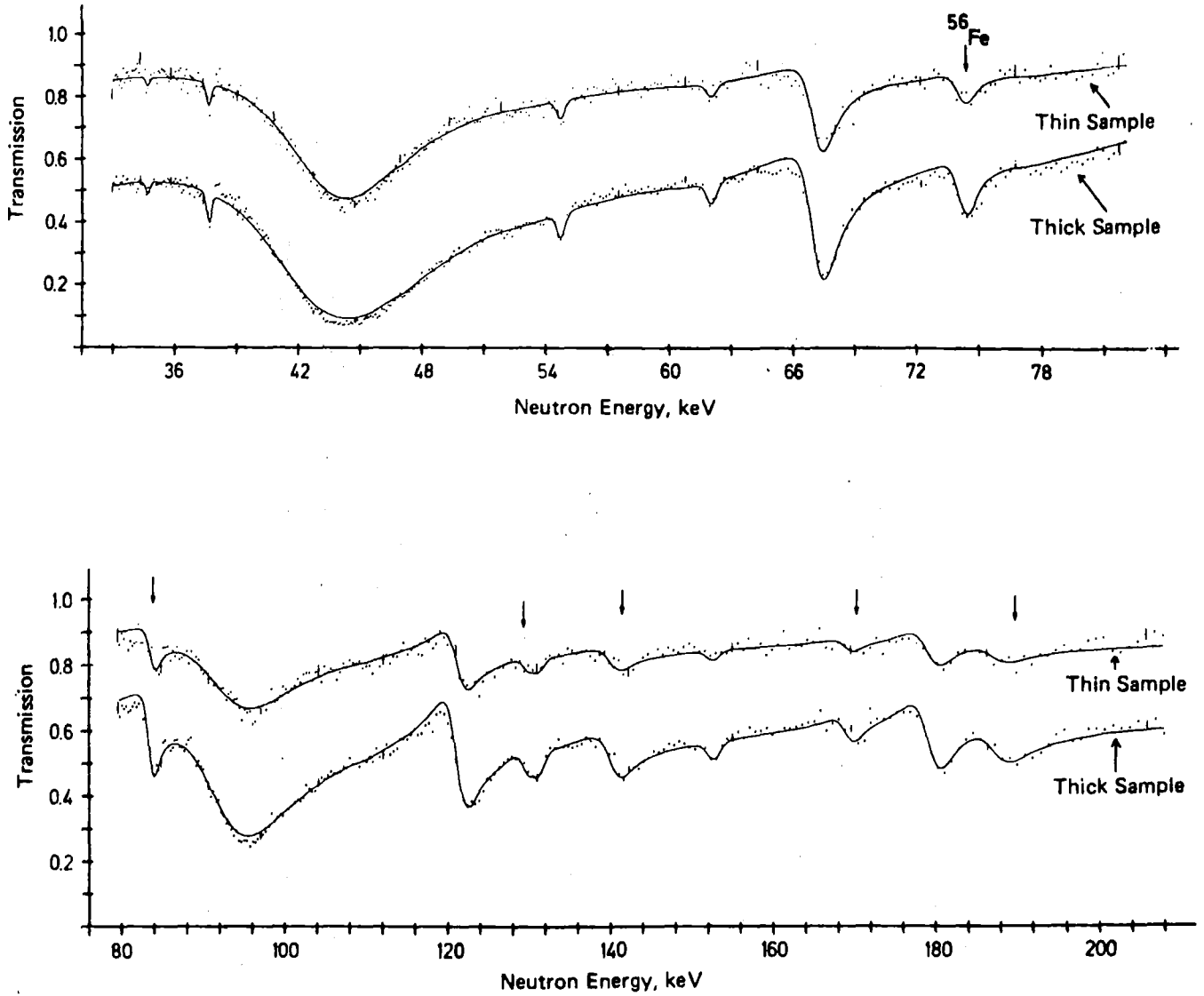


Fig. 7 - Thin- and thick-sample transmission data measured with  $\text{Fe}_2\text{O}_3$  samples containing 65.1 %  $^{58}\text{Fe}$ , 30.8 %  $^{56}\text{Fe}$ , 2.7 %  $^{57}\text{Fe}$  and 1.4 %  $^{54}\text{Fe}$ . The curves represent a simultaneous multi-level R-matrix fit obtained with the FANAL code (Ref. 12). The figure is taken from Ref. 8.

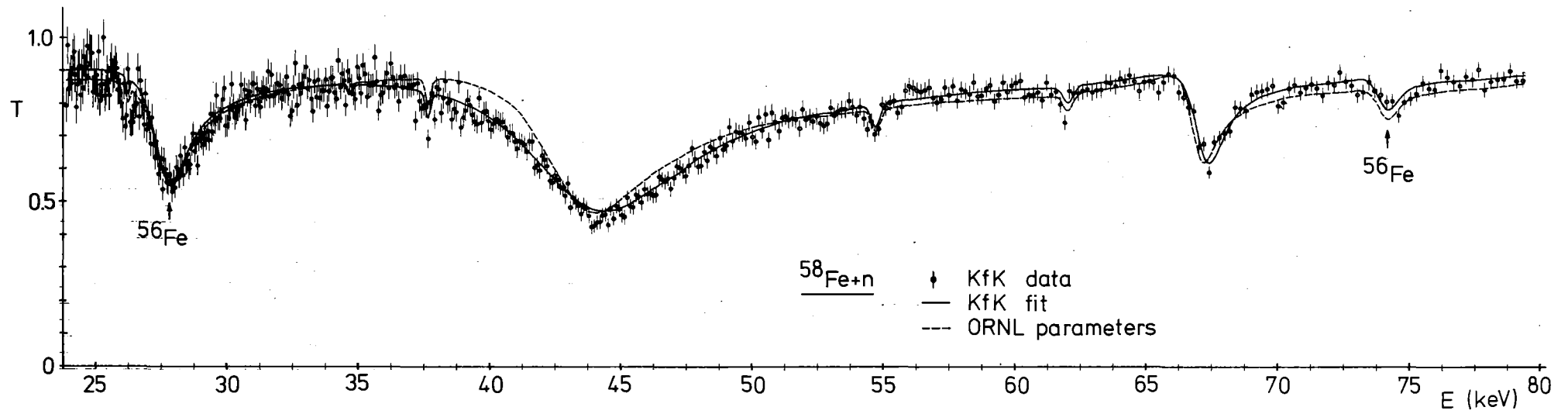


Fig. 8 - Comparison between KfK transmission data (0.0396 at./b  $\text{Fe}_2\text{O}_3$  with 65 %  $^{58}\text{Fe}$ , 31 %  $^{56}\text{Fe}$ ) and theoretical curves calculated with the KfK parameters (solid line) and Albany/ORNL parameters (dashed line) listed in Table 3.

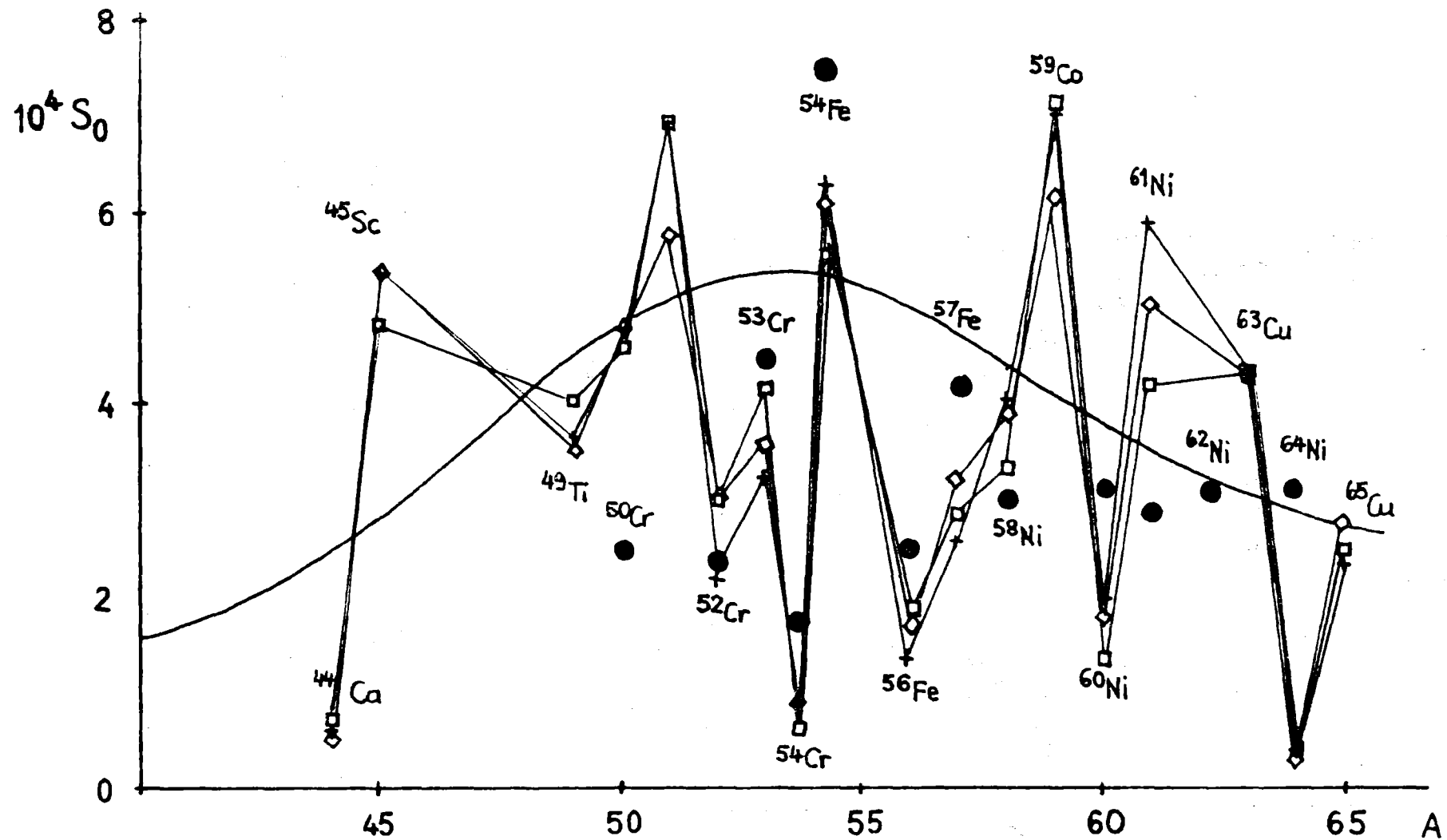


Fig. 9 - Strength function vs. nucleon number. Solid circles: revised STARA results; smooth curve: Buck and Percy, spherical optical model; other symbols: Müller and Rohr, statistical theory of doorway states.

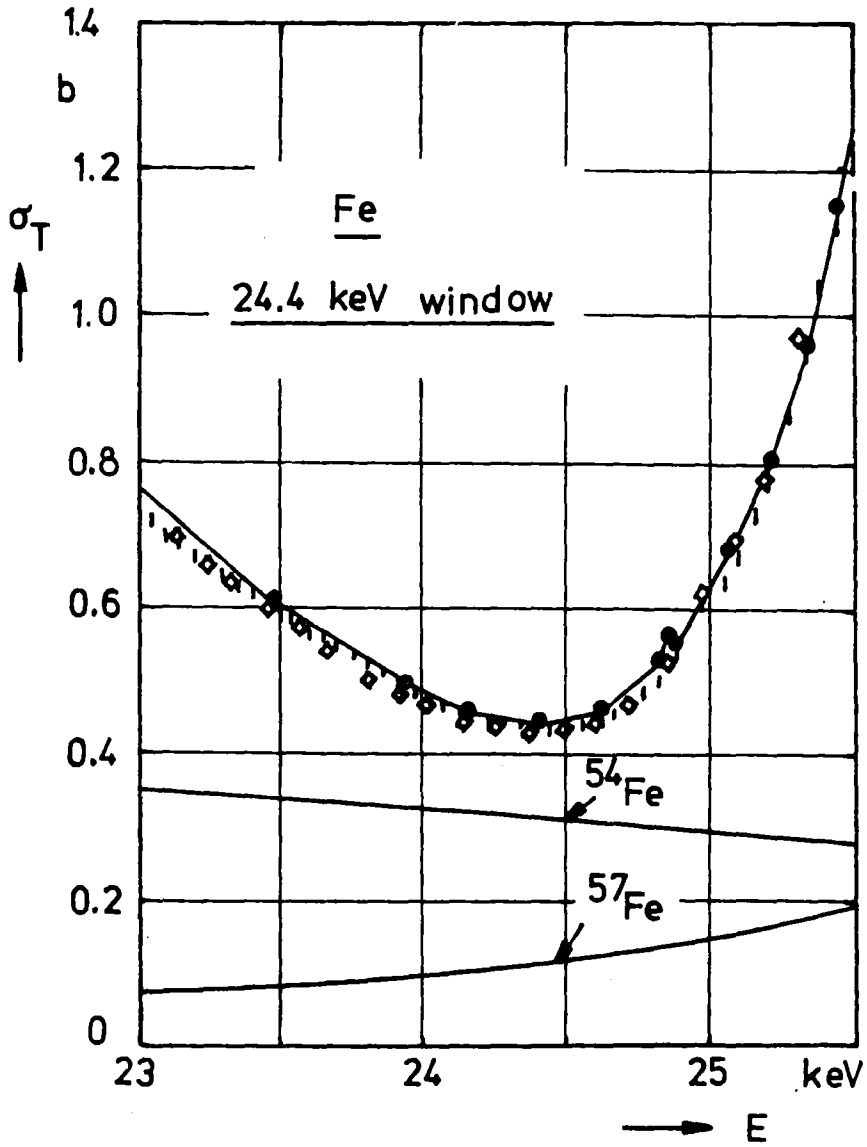


Fig. 10 - Comparison of total cross sections for natural iron across the 24.4 keV window.

- ◇ ◇ ◇ calculated with new data of Liou et al. for  $^{56}\text{Fe}$ , Ref. 17
- measured by Harvey, Ref. 18
- — ● KEDAK point data, calculated from evaluated resonance parameters, Ref. 3